Neurobiology of Aging 147 (2025) 176–186

Contents lists available at ScienceDirect

Neurobiology of Aging

journal homepage: www.elsevier.com/locate/neuaging.org

# Blood-brain barrier water permeability across the adult lifespan: A multi-echo ASL study

Beatriz E. Padrela [a,b,*], Maksim Slivka [c], Markus H. Sneve [c], Pablo F. Garrido [c,d], Mathijs B.J. Dijsselhof [a,b], Tamara Hageman [a], Oliver Geier [c,d], Håkon Grydeland [c], Amnah Mahroo [e], Joost P.A. Kuijer [a,b], Simon Konstandin [e,f], Klaus Eickel [e,f], Frederik Barkhof [a,b,g], Matthias Günther [e,h,i], Kristine B. Walhovd [c,j], Anders M. Fjell [c,j], Henk J.M.M. Mutsaerts [a,b], Jan Petr [a,k]

[a] Department of Radiology and Nuclear Medicine, Amsterdam Neuroscience, Amsterdam University Medical Center, Location VUmc, Amsterdam, the Netherlands
[b] Amsterdam Neuroscience, Brain Imaging, Amsterdam, the Netherlands
[c] Center for Lifespan Changes in Brain and Cognition, Department of Psychology, University of Oslo, Norway
[d] Department of Physics and Computational Radiology, Clinics of Radiology and Nuclear Medicine, Oslo University Hospital, Oslo, Norway
[e] Fraunhofer Institute for Digital Medicine MEVIS, Bremen, Germany
[f] Bremerhaven University of Applied Sciences, Bremerhaven, Germany
[g] Queen Square Institute of Neurology and Centre for Medical Image Computing (CMIC), University College London, London, UK
[h] mediri GmbH, Heidelberg, Germany
[i] Faculty 1 - Physics / Electrical Engineering, University Bremen, Bremen, Germany
[j] Computational Radiology and Artificial Intelligence, Clinics of Radiology and Nuclear Medicine, Oslo University Hospital, Oslo, Norway
[k] Helmholtz-Zentrum Dresden-Rossendorf, Institute of Radiopharmaceutical Cancer Research, Dresden, Germany

ARTICLE INFO

*Keywords:*
Blood-brain barrier
Water permeability
Arterial spin labeling
Cerebral blood flow
Aging
Magnetic resonance imaging

ABSTRACT

An emerging biomarker of blood-brain barrier (BBB) permeability is the time of exchange (Tex) of water from the blood to tissue, as measured by multi-echo arterial spin labeling (ASL) MRI. This new non-invasive sequence, already tested in mice, has recently been adapted to humans and optimized for clinical scanning time. In this study, we studied the normal variability of Tex over age and sex, which needs to be established as a reference for studying changes in neurological disease. We evaluated Tex, cerebral blood flow (CBF) and arterial transit time (ATT) in 209 healthy adults between 26 and 87 years, over age and sex, using general linear models in gray matter, white matter, and regionally in cerebral lobes. After QC, 194 participants were included in the main analysis, and the results demonstrated that both gray matter (GM) and white matter (WM) BBB permeability was higher with higher age (Tex lower by 0.47 ms per year in GM [$p < 0.05$], and by 0.49 ms in WM, for females; no significant for males), with the largest Tex difference in the frontal lobes (0.64 ms decrease per year, $p = 0.011$, population average). CBF was lower with higher age in the GM (-0.71 mL/min/100g per year, $p < 0.001$, for females; −0.31 mL/min/100g per year, $p < 0.05$, for males). When correcting Tex models for CBF and ATT, effect of age on Tex disappears in the GM, but not in the WM ($\beta$=-0.28, $p = 0.08$). The CBF findings of this study are in line with previous studies, demonstrating the validity of the new sequence. The BBB water permeability variation over age and sex described in this study provides a reference for future BBB research.

## 1. Introduction

The blood-brain barrier (BBB) is a semipermeable cellular barrier that plays a key role in maintaining brain homeostasis (Daneman and Prat, 2015; Weiss et al., 2009) and is involved in cerebrovascular dysfunction and inflammatory processes (Nation et al., 2019; Bowman

*Abbreviations:* ASL, Arterial spin labeling; ATT, Arterial transit time; BBB, Blood-brain barrier; CBF, Cerebral blood flow; DCE, Dynamic contrast-enhanced; DW, Diffusion-weighted; GBCA, Gadolinium-based contrast agents; GM, Gray matter; MMSE, Mini-Mental Status Examination; PLD, post label delay; SBD, sub-bolus duration; Tex, time of exchange; WM, White matter.

* Correspondence to: Department of Radiology and Nuclear Medicine, Amsterdam UMC, PK −1X 100, De Boelelaan 11, Amsterdam 171182 DB, the Netherlands.
*E-mail address:* b.estevespadrela@amsterdamumc.nl (B.E. Padrela).

https://doi.org/10.1016/j.neurobiolaging.2024.12.012
Received 13 August 2024; Received in revised form 28 November 2024; Accepted 29 December 2024
Available online 7 January 2025
0197-4580/© 2024 Published by Elsevier Inc.

et al., 2018). It was already reported in the 1970s that, in aging, the BBB structure becomes compromised (Tibbling, Link, and Ohman, 1977), and various studies have investigated possible causes of this breakdown with aging (Hussain, Fang, and Chang, 2021). A special focus has been given to the role of astrocytes and alterations in aquaporin-4 (AQP4) expressions, and both have been related to the accumulation of amyloid-β in the brain in animal models (W. Yang et al., 2012; J. Yang et al., 2011; Kress et al., 2014) and humans (Hoshi et al., 2012; Zeppenfeld et al., 2017). Further supported by the mounting interest in the role of cerebrovascular pathology in the development and progression of Alzheimer's Disease (AD) (Sweeney et al., 2019; Aslanyan et al., 2024), efforts have been made to assess the BBB dysfunction in aging (Moyaert et al., 2023) and as a marker of microvascular damage in AD and other dementias.

Many challenges have emerged when trying to measure BBB permeability in a non-invasive and reliable way while also providing regional information (Skillbäck et al., 2017) and remaining clinically implementable (Elschot et al., 2021). Dynamic contrast-enhanced (DCE) MRI using gadolinium-based contrast agents (GBCA) allows for the assessment of regional information in a clinical setting and can provide quantitative maps of metrics reflecting BBB leakage. Due to their small molecular size, GBCAs can potentially outperform other molecules when studying earlier stages of BBB integrity. However, concerns persist about the potential GBCA effects on patients and the environment (Ramalho et al., 2017) and its cost-benefit ratio (Wamelink et al., 2024). As a result, research is now shifting towards simpler and GBCA-free methods based on assessing BBB integrity through its permeability to water. This primarily includes advanced arterial spin labeling (ASL) approaches, which are techniques that measure perfusion non-invasively by magnetically labeling blood in brain-feeding arteries and subsequently imaging the delivery of the labeled blood into the brain parenchyma.

Traditionally, ASL measurements are quantified using a single-compartment model that, within a voxel, combines the signal from intra- or extravascular compartments (Clement et al., 2022). These two signal sources of the water molecules in the blood vessels and capillaries or in the interstitial fluid can be distinguished by either their different magnetic properties or diffusivity based on multi-echo time or diffusion-weighted (DW) measurements, respectively. Multi-echo ASL utilizes the difference in T2 relaxation time of labeled water molecules in the two compartments (longer in capillary and shorter in tissue) (Gregori et al., 2013), whereas DW-ASL uses their distinctive diffusivity (higher in capillary and lower in tissue) (Shao et al., 2019). These two concepts allow for the estimation of the labeled water exchange time (Tex) between the compartments to quantify the BBB permeability to water in each voxel. To understand BBB alterations in neurodegenerative diseases, it is essential to first understand the normal variability of BBB permeability, its relationship with age and sex, and the potential influences of other hemodynamic parameters on ASL-based BBB measurements.

Pilot studies tested the reproducibility (Mahroo et al., 2021) and the feasibility of BBB mapping with multi-echo ASL in the context of aging and neurodegeneration (Ohene et al., 2019), and early healthy aging results are available in mice (Ohene et al., 2020) and in humans (Mahroo, Konstandin, and Günther, 2023). While age-related variations were demonstrated in all studies, the direction and magnitude of the permeability differences are inconsistent (Gold et al., 2021; Ohene et al., 2020), likely owing mainly to differences in characteristics of the studied populations, small sample sizes, and the use of different acquisition techniques. Furthermore, BBB-ASL quantification relies on the delivery of labeled blood to the site of exchange. This can be potentially influenced by other hemodynamic parameters measured with ASL, such as cerebral blood flow (CBF) and arterial transit time (ATT), which are also known to have high physiological variability over age and sex across healthy volunteers (Holme et al., 2023; Vidyasagar et al., 2013). The multi-echo BBB-ASL developed in the "DEveloping BBB-ASL as non-Invasive Early biomarker" (DEBBIE) project (Mahroo et al., 2021; Padrela et al., 2024) allows both ATT and CBF estimation through a multi-post labeling delay (PLD) protocol and is potentially better able to deal with confounding effects of the heterogeneous blood delivery. Compared to other BBB-ASL such as DW-ASL, the main advantage of multi-TE BBB-ASL MRI is acquisition time. DW-ASL needs multiple b-value acquisitions and the latest multi-PLD implementation has a total acquisition time of 35 min (Shao et al., 2023). The DEBBIE multi-TE BBB-ASL with time-encoded labeling achieves reasonable quality within clinically feasible scanning time (<7 min), making it more suited for addition to larger population studies.

In this study, we aim to establish the normal variation of BBB Tex across age and sex for this novel DEBBIE sequence in 209 cognitively non-impaired participants acquired across the age range 26–87 years. To validate our sequence, we also studied the age and sex variation in CBF, a well-established parameter that can affect Tex quantification. We aimed to answer the following research questions: 1) What are the global and regional associations of Tex and CBF with age and sex? 2) Are the Tex associations influenced by other ASL-derived hemodynamic parameters and their image quality?

## 2. Material and methods

### 2.1. Study participants

Data from 218 cognitively unimpaired healthy participants were drawn from a longitudinal study running since 2006 at the Center for Lifespan Changes in Brain and Cognition (LCBC) at the University of Oslo, where participants had been followed for many years. BBB-ASL scans were added to the MRI protocol in June 2022, and the current study sample includes data collected until September 2023, encompassing all participants invited for a follow-up session during this period. The baseline exclusion criteria included sequelae and diagnosis of dementia, Parkinson's disease, and other neurodegenerative diseases likely to affect cognition (Wang et al., 2022). At the follow-up visit, we drew the scans for the current study, and the structural scans were checked by a neuroradiologist to exclude the occurrence of new major pathology, including presence of infarcts or other vascular conditions. Only participants older than 50 had a Mini-Mental Status Examination (Tombaugh and McIntyre, 1992). Following the quality control described below, a total of 194 subjects were included in the main analysis. Demographics of the included 194 participants can be found in Table 1.

### 2.2. Image acquisition

#### 2.2.1. MRI

MRI data were acquired at a 3 T system (MAGNETOM Prisma, Siemens Healthineers, Erlangen, Germany) with a 32-channel head coil. (Gregori et al., 2013; Mahroo et al., 2021). A 3D T1-weighted Magnetization Prepared RApid Gradient Echo (MPRAGE) image was acquired with the following parameters: TR = 2400 ms, TE = 2.22 ms, inversion time (TI) = 1000 ms, flip angle = 8°, FOV = 256 x 240 $mm^2$, spatial resolution = 0.8×0.8×0.8 $mm^3$, matrix size = 320 x 300, number of slices = 208, AC-PC aligned sagittal orientation, and scan duration = 6:38 min. BBB-ASL data were acquired with a combination of two multi-echo Hadamard (HAD) pseudo-continuous (PCASL) sequences (Mahroo et al., 2021) with a 3D Gradient and Spin Echo (GRASE) (Günther, Oshio, and Feinberg, 2005) readout. The first sequence (HAD8) was optimized for CBF and ATT estimation and was acquired using an 8×8 Hadamard matrix with a sub-bolus duration (SBD) of 400 ms and two repetitions with PLDs = [600, 1000, 1400, 1800, 2200, 2600, 3000] ms and PLDs = [800, 1200, 1600, 2000, 2400, 2800, 3200] ms, respectively, echo time (TE) = 13.4 ms, repetition time (TR) = 4190 ms, turbo factor = 12, one GRASE segment, spin-echo refocusing flip angle = 120°, and scan duration = 2:18 min. The second sequence was optimized for Tex estimation and was acquired using a 4×4

**Table 1**
Study sample demographics.

| | Female (n = 131) | Male (n = 63) | Sex difference (p-value) | All participants (n = 194) |
|---|---|---|---|---|
| **Age (y)** | | | | |
| Mean (SD) | 49.3 (14.5) | 51.4 (16.6) | 0.391 | 49.9 (15.2) |
| **Years of education** | | | | |
| Mean (SD) | 16.9 (2.5) | 16.4 (3.1) | 0.314 | 16.7 (2.7) |
| **MMSE** | | | | |
| Mean (SD) | 28.8 (1.26) | 29.1 (1.06) | 0.318 | 28.9 (1.20) |
| **Blood pressure** | | | | |
| Systolic: Mean (SD) | 134.1 (11.8) | 130.5 (28.4) | 0.86 | 132.3 (19.5) |
| Diastolic: Mean (SD) | 80.1 (6.57) | 81.1 (9.90) | 0.89 | 80.61 (7.53) |
| **BMI** | | | | |
| Mean (SD) | 25.41 (5.91) | 25.02 (3.02) | 0.699 | 25.31 (5.35) |
| **GM volume (mL)** | | | | |
| Mean (SD) | 632 (56.5) | 685 (76.1) | < 0.001 | 651 (68.8) |
| **WM volume (mL)** | | | | |
| Mean (SD) | 501 (51.3) | 562 (67.3) | < 0.001 | 523 (64.4) |
| **WMH volume (mL)** | | | | |
| Mean (SD) | 3.89 (5.91) | 6.24 (8.57) | 0.05 | 4.65 (6.95) |

ATT: Arterial transit time; BMI: body-mass index; CBF: cerebral blood flow; MMSE: Mini-Mental State Examination; GM: gray matter; SD: standard deviation; Tex: time of exchange; WM: white matter; WMH: white matter hyperintensities.

Hadamard matrix with an SBD of 1000 ms, PLD = [500, 1500, 2500] ms, eight TEs = [14:28:210] ms, TR = 4670 ms, two repetitions, turbo factor 2, six GRASE segments, spin-echo refocusing flip angle = 180°, and scan duration = 3:49 min. Two frequency offset corrected inversion (FOCI) pulses timed to suppress signal contributions with T1 values of 700 ms and 1400 ms were used for background suppression. A separate M0 image was acquired with a TI = 2300 ms, TR = 5000 ms, TE = 13.4 ms, turbo-factor = 12, spin-echo refocusing flip angle = 120°, and scan duration = 0:35 min. All PCASL measurements (HAD8, HAD4, M0) were acquired with the in-plane field of view (FOV) = 320 x 160 $mm^2$ and shared these common parameters: spatial resolution = 5x5x5 $mm^3$, matrix size = 64 x 128, number of slices = 24, echo-planar imaging (EPI) factor = 16, slice partial Fourier = 6/8, one pre-scan, bandwidth = 2298 Hz/Px, and acceleration of 2×2 with Controlled Aliasing in Parallel Imaging Results in Higher Acceleration (CAIPIRINHA). The scan duration of ASL and M0 sequences together was 7 min.

### 2.3. Image processing

Data were analyzed with ExploreASL (Henk J. M. M. Mutsaerts et al., 2020a and 2020b) version 1.11 using default settings. This included segmentation and spatial normalization of the T1-weighted images to the MNI space with CAT12, as well as registration of ASL to T1-weighted images. Motion correction was applied to realign all raw ASL images before Hadamard decoding to the first image. Motion estimation was performed on the first echo and applied equally to all echoes. Data from both sequences were quantified at once to obtain all parameters – CBF, ATT, and Tex – in a single fit. CBF, ATT, and Tex maps were quantified voxelwise with FSL-FABBER version 6.0.4 adapted to Tex quantification (Mahroo et al., 2021; Chappell et al., 2009). The values used for blood T1, tissue T1, blood T2 and tissue T2 were were 1664, 1331, 165, and 85 msec, respectively, taken from the literature ("Magnetic Resonance Imaging of the Brain and Spine, 4th Ed., Vol. 1 and 2" 2009; Mahroo, Konstandin, and Günther, 2023).

#### 2.3.1. Quality Control (QC)

The quantified maps were visually checked for motion artifacts and alignment with the T1-weighted images. Participants with motion artifacts or misalignment after processing were excluded. For inclusion of scans, first the automatic QC of ExploreASL was used, which ranks scans by their spatial coefficient of variation (CoV) (Mutsaerts et al., 2017), reflecting the amount of arterial transit time artefacts. After excluding the worst quality scans (unusable) by visual assessment, all remaining scans were categorized into: 1) 'Good' (CoV $\leq$ 0.6, cerebral blood flow signal predominates artefacts); 2) 'Acceptable' (0.6 $\leq$ CoV $\leq$ 0.8, both cerebral blood flow signal and artefacts visible); or 3) 'Vascular' (CoV > 0.8, artefacts predominate cerebral blood flow signal). Two authors (B. E.P. and J.P.), with, respectively, 3 and 10 years of experience in handling ASL data, independently reviewed and corrected the sCoV-based categorization of the images. Inconsistencies were resolved by consensus.

#### 2.3.2. Regions-of-interests (ROIs)

Two ROI masks were created by taking the entire segmented GM (total GM) and by eroding the segmented WM to reduce the GM content (deep WM) (Henri J. M. M. Mutsaerts et al., 2014). An example of a deep WM mask is shown in Supplementary Figure 1. In addition, we used the following ROIs for different analyses calculated as an intersection of the total GM mask with anatomical masks in the MNI space: four ROIs corresponding to the cerebral lobes — frontal, parietal, temporal, and occipital — and three ROIs consisting of the vascular territories supplied by the anterior (ACA), middle (MCA), and posterior cerebral arteries (PCA) (H. J. M. M. Mutsaerts et al., 2015). The model-fitted voxel-wise values of Tex and CBF were evaluated across the ROIs. All ROI values were also individually partial-volume corrected (PVC) using the segmented GM and WM maps (Asllani, 2008). The high-resolution GM/WM maps were smoothed to the effective ASL resolution prior to using them for PVC (Petr et al., 2018; Vidorreta et al., 2014).

### 2.4. Statistical analysis

All analyses were done by including participants with scans labeled as Good and Acceptable quality only. A two-sample *t*-test was conducted to determine if there was a statistically significant difference in CBF values between males and females. Then, we performed general linear models (GLM) to investigate the associations between Tex over age and sex in the same model but separately for all ROIs. We also performed a sensitivity analysis to address the issue of multiple comparisons by applying False Discovery Rate (FDR) correction (Benjamini and Hochberg, 1995). Additionally, we included the participants labeled with 'Vascular' CBF maps and repeated these models to understand the effect of QC on the analysis. We also investigated the correlation between GM and WM ATT with GM and WM CBF and Tex, respectively.

Furthermore, we extended the GLM assessing the total GM and deep WM ROIs to include the effect of CBF and ATT on Tex. To validate our ASL sequence in comparison with existing literature, we also performed GLM to study the effect of age and sex on total GM and deep WM CBF. Then, the effect of PVC was studied for this sequence (Asllani et al., 2009; Clement et al., 2017). To investigate the effect of GM volume differences across age and sex, we repeated the GLMs with partial volume corrected (PVC) Tex and CBF (Asllani, Borogovac, and Brown, 2008), taking into account the influence of age and sex from the previous model. Finally, to study the possible effect of T2 changes over age, we have performed a sensitivity analysis using age-based T2 values from the literature. All statistical analyses were performed in R Statistical Software (v4.3.2; R Core Team 2023), and $p < 0.05$ was considered statistically significant.

## 3. Results

### 3.1. Study sample characteristics

Out of the 218 participants, 9 participants were excluded from the analysis due to visible head motion. Among the 209 participants included in the analysis, 74 participants were classified as having CBF maps with "Good" quality, 120 as "Acceptable," and 15 as "Vascular" (Figure 1A). There seems to be a dependency of quality on age, with most of the "Vascular" CBF maps coming from participants over 60 years of age and most "Good" CBF maps from participants below 60 years of age (Figure 1B). Acceptable" CBF maps were spread throughout the age span. Finally, a total of 194 participants (Table 2) between 27 and 87 years, 67 % female, QC-labeled as "Good" or "Acceptable" were included in the analyses. Supplementary Table 1 includes the demographics description of all age groups. According to literature (Klatsky et al., 2017), normal BMI goes from 18 to 24.9 and then from 25–29 overweight, and since our values have an average of 25.4, they can be considered somehow in the threshold / slightly overweight. Regarding BP, high BP is considered above 140 mm, so since our sample participants have a total average BP of 132.

### 3.2. Tex and CBF associations over age and sex

Table 3 shows Tex and CBF variation across age, sex, and their interactions. Tex values are significantly dependent both on sex and age in GM and deep WM before PVC (Table 3A), but no significant interaction effect between age and sex was observed. Table 3B indicates that GM CBF significantly varied with age and sex, with and without PVC, and WM CBF also varied with sex. The interaction effect is significant only in GM CBF, both with and without PVC. In Supplementary Table 2, we repeated these analyses, including the participants that had 'Vascular' CBF maps (n = 15), and the age-related decrease in Tex and CBF became stronger for both sexes. After PVC, age effects remained only in CBF, with a non-significant Tex decrease in females and a non-significant Tex increase in males.

When studying GM Tex and CBF over age for males and females, we observed that Tex was lower at higher ages than at younger ages for females, while in the male sample, Tex was relatively stable across the age groups (Figure 2A). Similarly for CBF, the slopes of CBF change with age differed between males and females (Figure 2B) — with females having a steeper negative slope when modeling CBF changes with age (Table 3B). Adjusting for age-corrected T2 and T1 values, Tex values over age resulted in the same effect with a higher magnitude (Supplementary Figure 2).

**Table 2**
Study sample ASL-derived metrics.

| | Female (n = 131) | Male (n = 63) | Sex difference (p-value) | All participants (n = 194) |
|---|---|---|---|---|
| **Total GM ATT (s)** | | | | |
| Mean (SD) | 1.126 (0.016) | 1.129 (0.015) | 0.09 | 1.127 (0.016) |
| **Total WM ATT (s)** | | | | |
| Mean (SD) | 1.176 (0.03) | 1.189 (0.04) | 0.02 | 1.180 (0.03) |
| **Total GM CBF (mL/100g/min)** | | | | |
| Mean (SD) | 81.3 (21.0) | 65.3 (16.2) | < 0.001 | 76.2 (20.9) |
| **Total WM CBF (mL/100g/min)** | | | | |
| Mean (SD) | 19.2 (5.9) | 15.9 (4.1) | < 0.001 | 18.1 (5.6) |
| **Total GM Tex (ms)** | | | | |
| Mean (SD) | 230 (39.2) | 193 (34.5) | < 0.001 | 218 (41.4) |
| **Total WM Tex (ms)** | | | | |
| Mean (SD) | 155 (33.2) | 135 (26.2) | < 0.001 | 149 (33.2) |

ATT: Arterial transit time; BMI: body-mass index; CBF: cerebral blood flow; MMSE: Mini-Mental State Examination; GM: gray matter; SD: standard deviation; Tex: time of exchange; WM: white matter; WMH: white matter hyperintensities.

Figures 3 and 4 present the average Tex and CBF maps, respectively, for each age group. The participants were divided into groups by decades, and the groups 20–30y and 80–90y were merged with the neighboring groups as they did not contain many participants. While CBF appears lower at higher ages similarly across all regions, Tex shows more differences in some regions than others, mostly in the frontal and parietal lobes (see arrows in Figure 3). Separate Tex and CBF maps for males and females across age groups show clear differences between males and females (Supplementary Figure 3 and 4). Age-related ATT increases are particularly clear in the PCA territory and the watershed regions (Supplementary Figure 5).

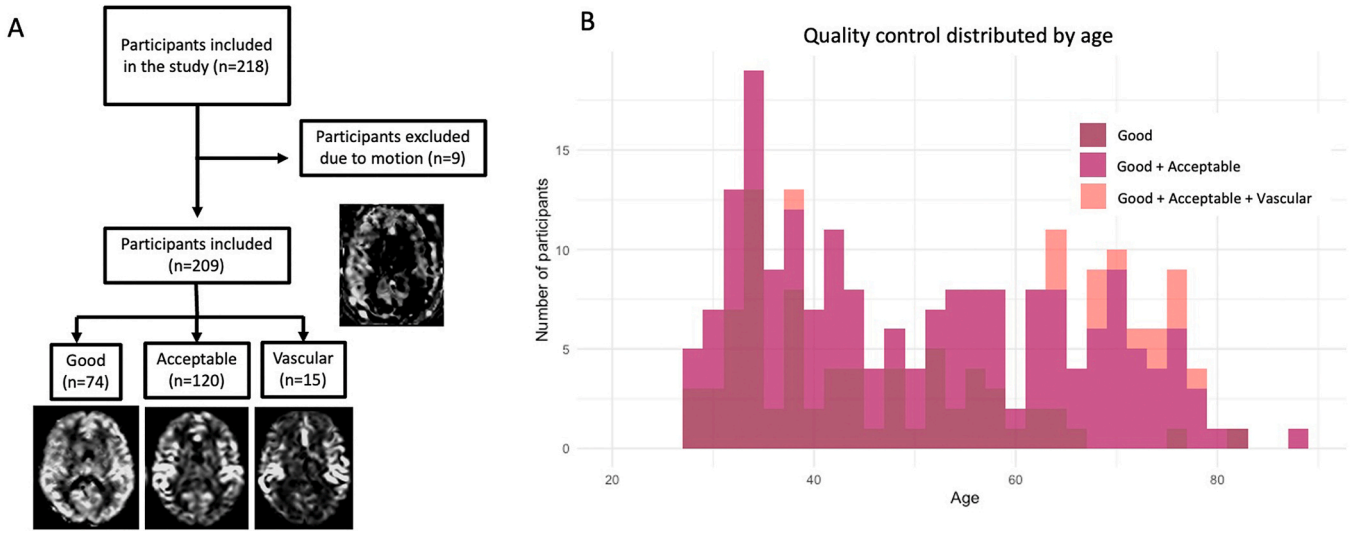


**Fig. 1.** Inclusion and exclusion of participants for analysis based on quality control of CBF maps (A) and age distribution of the quality labels (B).

**Table 3**
Tex (A) and CBF (B) GLM models of age and sex for GM and WM, with and without partial volume correction.

| A | Tex ~ Age + Sex + Age*Sex | | | | | |
|---|---|---|---|---|---|---|
| | Age | | Sex | | Age* Sex | |
| **Tex (ms)** | ***β*** | ***p*** | ***β*** | ***p*** | ***β*** | ***p*** |
| GM | −0.42 | 0.025* | −45.41 | 0.012* | 0.39 | 0.243 |
| WM | −0.49 | 0.009** | −43.90 | 0.008** | 0.48 | 0.119 |
| PVC GM | −0.22 | 0.453 | −62.36 | 0.012* | 0.58 | 0.212 |
| PVC WM | −0.37 | 0.081 | −47.81 | 0.009** | 0.59 | 0.083 |
| B | CBF ~ Age + Sex + Age*Sex | | | | | |
| | Age | | Sex | | Age* Sex | |
| **CBF(mL/100g/min)** | ***β*** | ***p*** | ***β*** | ***p*** | ***β*** | ***p*** |
| GM | −0.72 | < 0.001 *** | −35.26 | < 0.001 *** | 0.41 | 0.027 * |
| WM | −0.05 | 0.144 | −7.78 | 0.006** | 0.08 | 0.090 |
| PVC GM | −0.95 | < 0.001 *** | −48.98 | < 0.001 *** | 0.43 | 0.033 * |
| PVC WM | 0.004 | 0.879 | −6.22 | 0.007** | 0.08 | 0.068 |

CBF: cerebral blood flow; GM: gray matter; WM: white matter; PVC: partial volume corrected; Tex: time of exchange. NB: the negative beta for sex indicates the value is smaller for males compared to females.
* $p < 0.05$;
** $p < 0.01$;
*** $p < 0.001$.

### 3.3. Regional values

Similarly to what was observed in the age-stratified Tex maps (Figure 2), Table 4A shows that Tex was significantly correlated with age in the frontal lobe, as well as with ACA and PCA vascular territories (ACA: $p = 0.032$, PCA: $p = 0.014$). The differences between sexes were evident in all regions except the occipital lobe ($p = 0.66$). The interaction between age and sex was similar in magnitude to the age effects; however, it was not significantly associated with Tex. Tex results did not survive multiple comparisons correction. On the other hand, CBF was significantly correlated with age and sex in all regions (Table 4B). The interaction between age and sex was significantly associated with CBF in the frontal and parietal lobes and both ACA and MCA territories.

We then investigated the Tex dependence on age, sex, ATT, and CBF (Table 5). Since the interaction term between age and sex was not significant in the first model (Table 3), we chose not to include it in this model to focus on the influence of these specific covariates.

We found that WM Tex is independently significantly associated with all studied parameters; however, GM Tex was associated with all parameters except for age ($p = 0.163$). Additionally, to investigate WMH influence on this model, we have added Supplementary Table 3 with WMH as a covariate, and the results do not change with respect to the model in Table 4 (minimal change of betas, significance not affected). In Supplementary Figures 6 and 7, we present plots of ATT versus CBF and ATT versus Tex for both GM and WM, respectively, to assess the influence of ATT on these metrics. These results suggest that ATT only correlates with WM CBF but it is not correlated with Tex.

## 4. Discussion

In this study, we observed that BBB Tex correlates negatively with age both in gray and white matter. Tex was lower in males than females overall, with the age-related Tex association most pronounced in the frontal lobe. In this work, Tex serves as a proxy of higher BBB water permeability. CBF was shown to be lower with higher age, in line with the literature, and affected by sex even after correcting for PVC. Finally, we found that correcting for CBF and PVC decreased the correlation of Tex with age but not with sex.

Our observation that total GM BBB water permeability (given by lower Tex) with higher age is consistent with previous smaller multi-echo ASL studies in both mice and humans (Ohene et al., 2020; Mahroo, Konstandin, and Günther, 2023). Although we cannot directly interpret the cause of the observed Tex effects from these results, several mechanisms have been proposed in the literature. The observed age-related decrease of Tex may be due to an increased expression of aquaporin-4 with aging (Zeppenfeld et al., 2017) or by aging-related pericyte deficiency (Armulik et al., 2010). On the other hand, dysfunctional pericytes can lead to a compromise in AQP4 polarization, reducing the concentration of these channels at the astrocytic end-feet and impairing water regulation (Armulik et al., 2010; Uemura et al., n.d.). The sensitivity of multi-echo ASL to measure water passage through AQP4 channels was demonstrated through lower BBB permeability in mice after blocking the AQP4 channels (Ohene et al., 2019). Notably, age-related Tex decreases were mostly similar between GM and WM, which was not the case for CBF, where GM CBF decreased more than WM CBF. Technically, ASL CBF quantification might be biased due to the presence of macrovascular signals, which are not fully accounted for in the model and are present for PLDs shorter than ATT. While no correlation was found between Tex and ATT or between GM CBF and GM ATT, WM CBF was correlated with WM ATT. This might explain slightly lower WM CBF than expected, but it cannot be concluded with the current data if this dependence is causal or if both values change

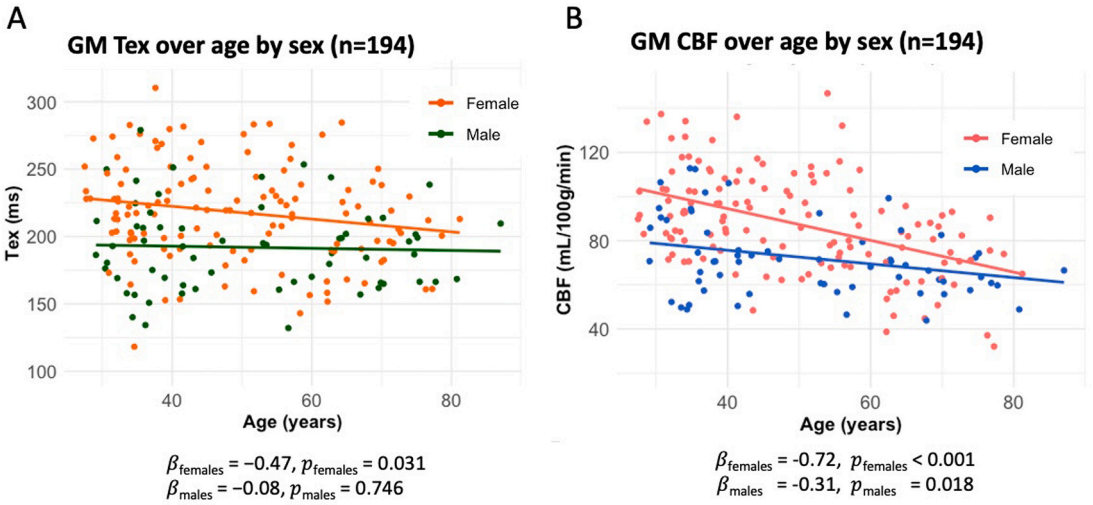


**Fig. 2.** Tex (A) and CBF (B) values over age stratified by sex. CBF: cerebral blood flow; GM: gray matter; Tex: time of exchange. β: estimated slope of the regression line, p: p-value.

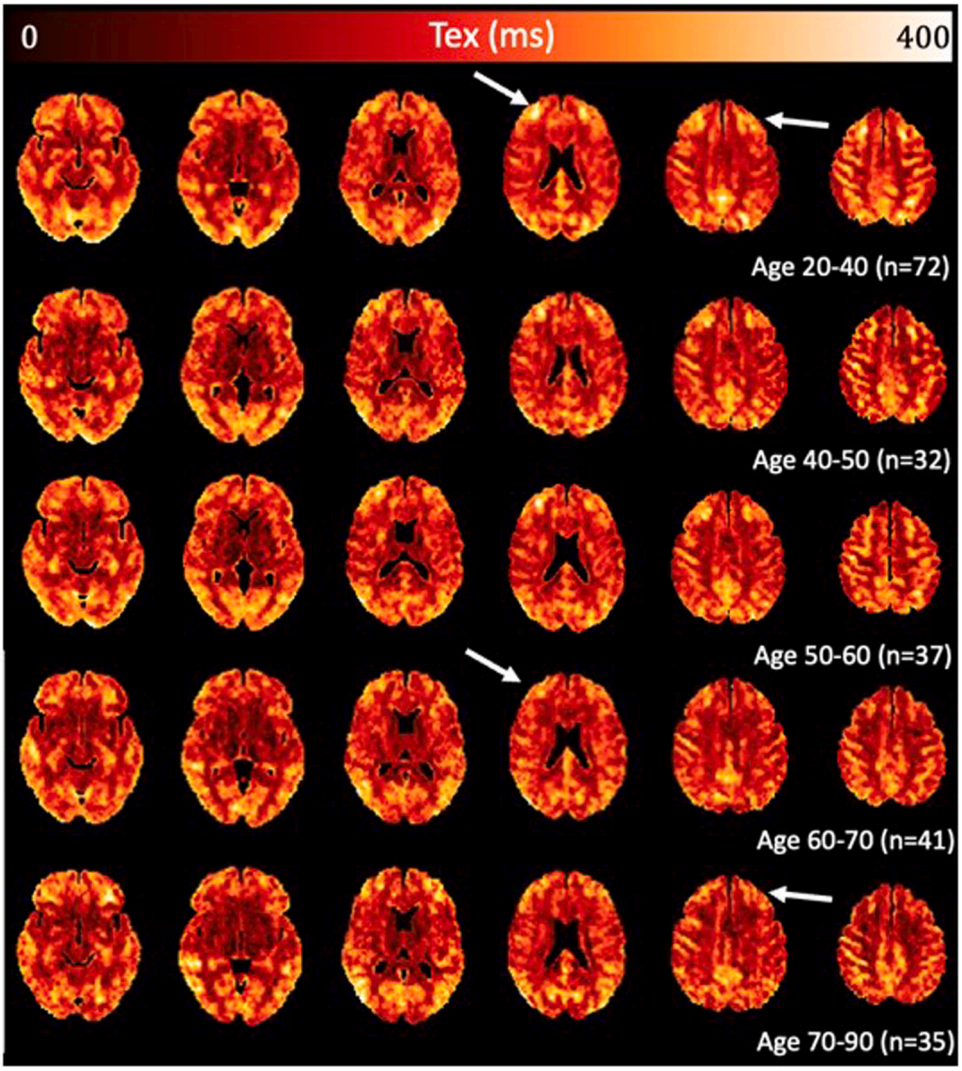


**Fig. 3.** Average Tex maps per age group (in years). The same scale was applied to all age groups. The arrows point to regions with the visually clearest intensity differences in the Tex maps across different age groups. Tex: time of exchange.

with age independently. From the physiological perspective, the similar Tex decrease in WM and GM attests to a comparable degradation of the microvasculature in all tissues. CBF changes with age seem to differ between GM and WM. Our results agree with other studies showing that GM CBF declines with age, perhaps due to aging-related loss of neuronal density(Staffaroni et al., 2019). Our finding of stable WM CBF across age has been already stated in literature(Han et al., 2022), suggesting that the WM might only require CBF for maintenance of the axons and supporting tissue, however, other studies have found negative(Biagi et al., 2007) or mixed associations that vary both by tract and by sex (Robinson et al., 2023) between WM CBF and age.

Our results show higher BBB water permeability (given by lower Tex) in males than in females, which aligns with previous DCE studies in humans (Moon et al., 2021) and can potentially be explained by genetic, hormonal, and lifestyle factors (Weber and Clyne, 2021). Many of these factors differ not only between sexes in general but have different aging patterns. E.g., genetic differences in immune function between sexes (Spolarics, 2007) or life-long fluctuations in hormone levels (Robison et al., 2019; Biagetti and Puig-Domingo, 2023). The interplay between sex and BBB function in aging might have implications on the sex-stratified treatment opportunities. Although the literature on sex differences in AQP4 channels remains limited, some studies(Solarz, Majcher-Maślanka, and Chocyk, 2021) have identified differences in AQP4 expression between males and females, primarily in the context of estrogen effects and early-life stress models, with biomolecular analysis. While these studies offer some insights into sex differences in AQP4 channel function, further research is required to determine whether these findings are applicable to humans and their potential implications.

Additionally, the pronounced water permeability increase with age in the frontal lobe aligns with previous studies that found higher BBB leakage in orbitofrontal and cingulate cortices in healthy adults across the lifespan using DCE-MRI (Inge C. M. Verheggen et al., 2020). Likewise, the frontal cortex is known to be vulnerable to normal and vascular aging-related deterioration and vascular cognitive impairment (Inge C. M. Verheggen et al., 2020; Lorenzini et al., 2022), suggesting the need to investigate this further in future studies. Altogether, these findings are promising for developing BBB-ASL as a vascular aging biomarker and encourage future studies to correlate BBB-ASL with biomarkers of small vessel disease, cognitive decline, and AD.

Accurate quantification of Tex relies on the presence of labeled blood in the imaging voxel and might thus be influenced by lower and missing labeled blood signal due to high ATT. Our results indicate that Tex is correlated with CBF, which can be explained by a direct causal effect or because both are susceptible to similar vascular aging-related effects (Hafdi et al., 2022; Goodall et al., 2018). The fact that age affects our regional Tex estimates differently than regional CBF values suggests that

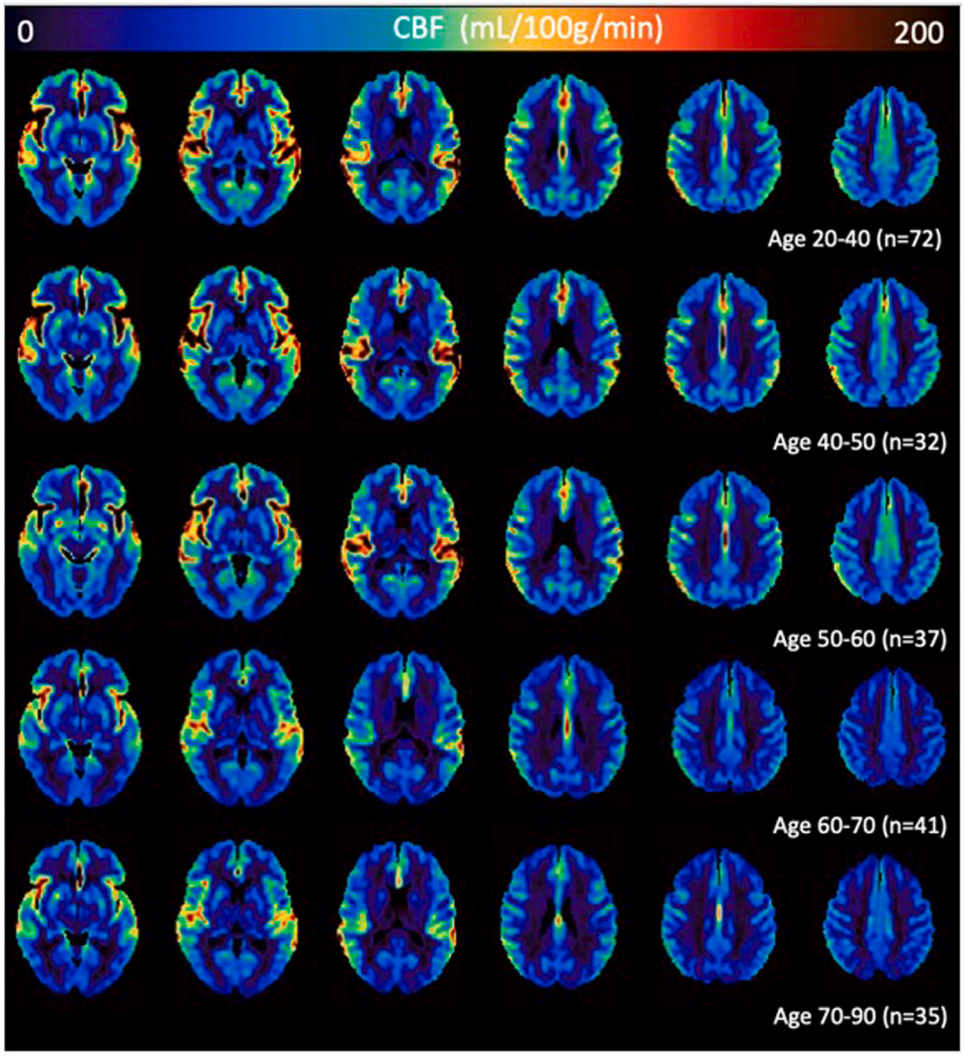


**Fig. 4.** Average CBF maps per age group (in years). The same scale was applied to all age groups. CBF: cerebral blood flow.

our Tex values are not predominantly confounded by CBF. A possible explanation for the correlation of Tex and CBF with age is that the vessel walls tend to stiffen, making them less able to accommodate pressure changes during the heart cycle, resulting in increased pressure fluctuation more distally in the vascular tree (Tarumi et al., 2009). Coupled with the overall higher incidence of hypertension in older age (Pinto, 2007), this could lead to BBB damage (Rosenberg, 2012; Setiadi et al., 2018), thereby reducing Tex along with decreased CBF. This could explain why we see the strongest association of ACA and PCA Tex with age, as their tissues have longer and more curved feeding vessels than the MCA territory. While the correlation between Tex and CBF across age was maintained when stratifying for sex, Tex decrease with age was more pronounced in women than in men, and future studies are encouraged to investigate the interaction of age and sex on hypertension and vascular aging and their effects on BBB water permeability and CBF.

Performing quality control is particularly important (Fallatah et al., 2018) as Tex quantification relies on labeling efficiency and the presence of sufficient ASL signal, which depends on ATT and prolongs with age (Mutsaerts et al., 2015; Y. Liu et al., 2012). While the cardio- and cerebrovascular risk factors in our population fall within the normal or expected range for a Norwegian aging population (Overweight and obesity in Norway), in our study, higher ATT correlated with a decrease in water permeability with age. Although this association cannot be interpreted as causal or confounding based on the current data, the age-related decrease in Tex and CBF are both reduced after removing the 'Vascular' scans, highlighting the importance of these thorough quality checks before analysis. Based on the fact that tissue ASL signal was largely missing in these participants and that larger vessels should not show permeability in healthy subjects, we can conclude that too long an ATT with respect to PLD and strong macrovascular signals leads to bias in Tex measurement. At the same time, older participants are more often excluded due to lower data quality (Woods et al., 2024), possibly further reinforcing the selection bias by studying only the healthier part of the older adults. However, current data does not allow us to investigate if the true cause of lower Tex is physiological and measurement-related, and further investigation with different modeling approaches is needed.

In line with the literature, our results show that GM CBF relates negatively to age, both with and without PVC (Juttukonda et al., 2021; Hu, Liu, and Gao, 2021; Asllani et al., 2009), and females show higher CBF values compared to males, especially in younger ages (Tomoto et al., 2023; W. Liu, Lou, and Ma, 2016). Surprisingly, the effect of the application of PVC — reducing the confounding effect of atrophy — differed between CBF and Tex. Whereas PVC resulted in a steeper GM CBF decrease over age, the age effect on Tex was reduced both in GM and WM. Noteworthy, a simple linear regression PVC method was performed to account for potential GM-WM tissue volume differences, which is common practice for CBF but has not been validated for Tex (Asllani, Borogovac, and Brown, 2008). Additionally, as an association was found between Tex and CBF, a tissue-specific CBF might improve the Tex quantification model and also the non-linearity in Tex

**Table 4**
Regional total GM Tex (A) and CBF (B) GLM models for cerebral lobes and the three vascular territories.

| A | Tex ~ Age + Sex + Age*Sex | | | | | |
|---|---|---|---|---|---|---|
| | Age | | Sex | | Age*Sex | |
| **Tex (ms)** | ***β*** | ***p*** | ***β*** | ***p*** | ***β*** | ***p*** |
| Frontal | −0.64 | 0.011* | −53.25 | 0.014* | 0.59 | 0.150 |
| Parietal | −0.21 | 0.422 | −53.94 | 0.018* | 0.54 | 0.204 |
| Temporal | −0.26 | 0.182 | −41.71 | 0.012* | 0.33 | 0.289 |
| Occipital | −0.48 | 0.136 | −50.22 | 0.066 | 0.18 | 0.727 |
| ACA | −0.50 | 0.032* | −49.54 | 0.013* | 0.49 | 0.195 |
| MCA | −0.34 | 0.109 | −47.05 | 0.011* | 0.49 | 0.154 |
| PCA | −0.72 | 0.014* | −61.93 | 0.013* | 0.38 | 0.421 |
| B | CBF ~ Age + Sex + Age* Sex | | | | | |
| | Age | | Sex | | Age* Sex | |
| **CBF (mL/100g/min)** | ***β*** | ***p*** | ***β*** | ***p*** | ***β*** | ***p*** |
| Frontal | −0.86 | $< 0.001^{***}$ | −42.71 | $< 0.001^{***}$ | 0.54 | 0.013* |
| Parietal | −0.69 | $< 0.001^{***}$ | −35.14 | $< 0.001^{***}$ | 0.38 | 0.041* |
| Temporal | −0.63 | $< 0.001^{***}$ | −28.89 | $0.002^{**}$ | 0.31 | 0.064 |
| Occipital | −0.72 | $< 0.001^{***}$ | −34.11 | 0.013* | 0.32 | 0.096 |
| ACA | −0.76 | $< 0.001^{***}$ | −39.25 | $0.003^{**}$ | 0.47 | 0.016* |
| MCA | −0.75 | $< 0.001^{***}$ | −36.93 | $< 0.001^{***}$ | 0.45 | 0.023* |
| PCA | −0.63 | $< 0.001^{***}$ | −30.38 | 0.0013* | 0.28 | 0.114 |

ACA: anterior cerebral artery; CBF: cerebral blood flow; MCA: middle cerebral artery; PCA: posterior cerebral artery; Tex: time of exchange.
* $p < 0.05$;
** $p < 0.01$;
*** $p < 0.001$.

quantification. The influence of both factors needs to be further studied in silico or in vitro to understand better the relation between PVC and Tex, possibly resulting in an extended model for Tex that includes PVC, which could offer more accuracy in future studies.

Interestingly, both multi-echo ASL and DW-ASL show clear changes in BBB water permeability over age, but the direction of change differs, with DW-ASL showing a decreased permeability with age (Ford et al., 2022; Gold et al., 2021; Shao et al., 2020). Note that the methods use different units. The Tex decrease in this study corresponds to increased tissue/capillary fraction (Kw), but previous DW-ASL studies found decreased Kw over age. The conflicting results of the two methods could be attributed to two processes happening simultaneously in normal aging – increased leakage through the tight junctions and decreased water transport due to dislocation of ~~through~~ the AQP4 channels (I. C. M. Verheggen et al., 2018). Due to a different mechanism of measurement, the two methods could be more sensitive to either of these effects. As discussed above, assessing Tex in older adults with ATT issues is challenging, especially using ASL sequences with single-PLD. The largest DW-ASL aging study that reports decreased permeability with age reported relatively stable permeability values across age, with the most important decline observed in individuals older than 70 years (Shao et al., 2024), using a single PLD that is relatively short for older adults. A possible source of discrepancy between this DW-ASL study and our study can thus be the single-PLD design (Lindner et al., 2023). A recent study has been published comparing these two methods(Morgan et al., 2024), stressing the differences between them. These findings stress the complexity of assessing BBB water permeability in older adults, encouraging future studies to investigate such confounding factors in greater detail and to introduce new quantification models.

Our study has some limitations. The first limitation is recruitment bias, which would apply to any MRI study of healthy volunteers. The older participants included in this study are likely healthier than the general population at the same age. This could result in less pronounced age-related effects in CBF and Tex, which should be considered when using the present data as a normative reference. Secondly, the low spatial resolution of ASL is a common challenge in ASL imaging, particularly when trying to get the best trade-off between scan time and signal-to-noise ratio (SNR). Despite these challenges, we obtained a sufficient number of good-to-medium quality ASL scans, allowing us to perform reliable linear regression analyses. Another limitation is that several parameters of the Tex and CBF quantification model may depend on age and sex, such as T1- and T2-times of the blood through their dependence on blood oxygenation and hematocrit levels (H.-S. Liu et al., 2019). However, developing an extended model to account for these changes was outside this work's scope, and fixed values of T1 and T2 relaxation times were used for all individuals for Tex quantification. Nevertheless, the sensitivity analysis using age-specific T2 values shows that the magnitude of changes across age is possibly higher when these literature reference values of blood and tissue relaxation times are used. As these group values come with high uncertainty, the use of subject-specific relaxation times could provide a more robust estimation of Tex values, which would require a multi-echo M0 or a quantitative T2 mapping and hematocrit measurements. Future studies should aim to incorporate these scans to improve precision. The current Tex quantification model does not consider non-capillary blood signals with lower permeability, like larger arteries, which can result in Tex overestimation, potentially biasing the Tex quantification across age. Likewise, the CBF image quality was judged by the number of macrovascular artifacts changed over age, with older adults having more vascular-appearing CBF maps even though a multi-PLD protocol was used. Furthermore, while the quantification model we used was specifically designed to account for the effects of ATT and intravascular transit time (ITT)(Mahroo et al., 2021), additional use of arterial blood volume estimations could potentially make this sequence more robust against vascular artifacts.

Finally, as there is currently minimal validation of BBB-ASL, assessing BBB permeability over the lifespan remains challenging. DCE is valuable for assessing regional BBB disruption, but its invasiveness has restricted large population studies of BBB permeability variability across the lifespan. Moreover, direct comparisons between water permeability (measured by BBB-ASL) and gadolinium permeability (DCE) are complex due to differing molecular weights and permeability profiles. For water permeability, a recognized gold standard in preclinical research compares 15O-H2O-PET with 11C-butanol PET, which we are currently investigating in pigs in a parallel study(Padrela et al., 2024). However, the invasiveness and high cost of 15O-H2O-PET make it difficult to validate BBB water permeability changes across the lifespan. Nevertheless, preclinical studies have validated the sensitivity of BBB-ASL to physiological changes; for example, Ohene et al. (2019)(Ohene et al., 2019) showed that multi-echo ASL can detect BBB permeability changes in mice with blocked AQP4 channels, confirming its sensitivity to alterations in water transport.

**Table 5**
Tex complete GLM model for GM and WM. ATT: arterial transit time; CBF: cerebral blood flow; GM: gray matter; Tex: time of exchange; WM: white matter.

| | Tex ~ Age + Sex + ATT + CBF | | | | | | | |
|---|---|---|---|---|---|---|---|---|
| | Age | | Sex | | ATT | | CBF | |
| **Tex (ms)** | ***β*** | ***p*** | ***β*** | ***p*** | ***β*** | ***p*** | ***β*** | ***p*** |
| GM | 0.21 | 0.163 | −11.43 | 0.016* | 410.94 | 0.006* | 0.97 | $< 0.001^{***}$ |
| WM | −0.28 | $0.008^{**}$ | −7.64 | 0.034* | 644.00 | $< 0.001^{***}$ | 3.73 | $< 0.001^{***}$ |

## 5. Conclusion

In summary, our study demonstrated increased BBB water permeability with age in a healthy adult lifespan sample alongside a consistently lower perfusion with age. It showed that BBB-ASL holds the potential for offering a direct and sensitive assessment of BBB Tex, which allows establishing reference values for detecting BBB changes in early disease stages. The regional and sex-related divergence in Tex adds further information to understanding healthy aging BBB, but these differences need to be established across samples. Additionally, these findings provide insight into image quality and the effects of confounders on Tex quantification, forming a basis for multi-echo BBB analysis. Overall, this article provides a reference for future research and increases our understanding of normal aging.

## CRediT authorship contribution statement

**Henk J.M.M. Mutsaerts:** Writing – review & editing, Writing – original draft, Supervision, Project administration, Methodology, Investigation, Conceptualization. **Tamara Hageman:** Formal analysis, Data curation. **Anders M. Fjell:** Writing – review & editing, Resources, Project administration, Investigation, Funding acquisition, Conceptualization. **Joost P.A. Kuijer:** Writing – review & editing, Software, Investigation. **Amnah Mahroo:** Writing – review & editing, Methodology, Investigation. **Håkon Grydeland:** Writing – review & editing, Validation, Resources, Methodology, Data curation. **Jan Petr:** Writing – review & editing, Writing – original draft, Validation, Supervision, Project administration, Methodology, Investigation, Conceptualization. **Oliver Geier:** Writing – review & editing, Software, Resources, Methodology, Data curation. **Matthias Günther:** Writing – review & editing, Resources, Funding acquisition. **Markus H. Sneve:** Writing – review & editing, Resources, Project administration, Methodology, Data curation, Conceptualization. **Frederik Barkhof:** Writing – review & editing, Methodology, Conceptualization. **Maksim Slivka:** Writing – original draft, Software, Resources, Data curation. **Klaus Eickel:** Writing – review & editing. **Beatriz E. Padrela:** Writing – review & editing, Writing – original draft, Methodology, Investigation, Formal analysis, Data curation, Conceptualization. **Simon Konstandin:** Writing – review & editing, Validation, Resources, Methodology, Investigation. **Mathijs B. J. Dijsselhof:** Writing – review & editing, Writing – original draft. **Kristine B. Walhovd:** Writing – review & editing, Supervision, Resources, Project administration, Methodology, Investigation, Funding acquisition, Conceptualization. **Pablo F. Garrido:** Writing – review & editing, Validation, Methodology.

## Declaration of Competing Interest

FB: Steering committee or Data Safety Monitoring Board member for Biogen, Merck, Eisai, and Prothena. Advisory board member for Combinostics, Scottish Brain Sciences, Alzheimer Europe. Consultant for Roche, Celltrion, Rewind Therapeutics, Merck, Bracco. Research agreements with ADDI, Merck, Biogen, GE Healthcare, and Roche. Co-founder and shareholder of Queen Square Analytics LTD.

## Acknowledgments

FB is supported by the NIHR biomedical research center at UCLH. The imaging acquisition was supported by the Norwegian Research Council (#325415 to H.G. and #325878 to A.M.F.). The DEBBIE project (Developing a non-invasive biomarker for early BBB breakdown in Alzheimer's disease) is an EU Joint Programme -Neurodegenerative Disease Research (JPND) project. It is supported through national funding organizations under the aegis of JPND -www.jpnd. The project has received funding from the European Union's Horizon 2020 research and innovation programme under grant agreement No. 825664 (BP, AM, JK, SK, KE, FB, MG, HJM, and JP are supported within DEBBIE).

*Verification*

We confirm that this work is performed in accordance with ethical standards, is original, and has not been published elsewhere, nor is it currently under consideration for publication elsewhere. This manuscript has been read and approved by all co-authors. The conflicts of interest are described in the 'Manuscript' document uploaded.

## Appendix A. Supporting information

Supplementary data associated with this article can be found in the online version at doi:10.1016/j.neurobiolaging.2024.12.012.

## References

"Magnetic Resonance Imaging of the Brain and Spine, 4th Ed., Vol. 1 and 2", 2009. Ajnr. Am. J. Neuroradiol. 30 (5), e76–e77. https://doi.org/10.3174/ajnr.a1553.

Armulik, Annika, Genové, Guillem, Mäe, Maarja, Nisancioglu, Maya H., Wallgard, Elisabet, Niaudet, Colin, He, Liqun, et al., 2010. Pericytes Regulate the Blood-Brain Barrier. Nature 468 (7323), 557–561. https://doi.org/10.1038/nature09522.

Aslanyan, Vahan, Mack, Wendy J., Ortega, Nancy E., Nasrallah, Ilya M., Pajewski, Nicholas M., Williamson, Jeff D., Pa, Judy, 2024. Cerebrovascular Reactivity in Alzheimer's Disease Signature Regions Is Associated with Mild Cognitive Impairment in Adults with Hypertension. Alzheimer'S. Dement.: J. Alzheimer'S. Assoc. 20 (3), 1784–1796. https://doi.org/10.1002/alz.13572.

Asllani, Iris, Borogovac, Ajna, Brown, Truman R., 2008. Regression Algorithm Correcting for Partial Volume Effects in Arterial Spin Labeling MRI. Magn. Reson. Med.: Off. J. Soc. Magn. Reson. Med. / Soc. Magn. Reson. Med. 60 (6), 1362–1371. https://doi.org/10.1002/mrm.21670.

Asllani, Iris, Habeck, Christian, Borogovac, Ajna, Brown, Truman R., Brickman, Adam M., Stern, Yaakov, 2009. Separating Function from Structure in Perfusion Imaging of the Aging Brain. Hum. Brain Mapp. 30 (9), 2927–2935. https://doi.org/10.1002/hbm.20719.

Benjamini, Yoav, Hochberg, Yosef, 1995. Controlling the False Discovery Rate: A Practical and Powerful Approach to Multiple Testing. J. R. Stat. Soc. Ser. B, Stat. Methodol. 57 (1), 289–300. https://doi.org/10.1111/j.2517-6161.1995.tb02031.x.

Biagetti, Betina, Puig-Domingo, Manel, 2023. Age-Related Hormones Changes and Its Impact on Health Status and Lifespan. Aging Dis. 14 (3), 605–620. https://doi.org/10.14336/AD.2022.1109.

Biagi, Laura, Abbruzzese, Arturo, Bianchi, Maria Cristina, Alsop, David C., Del Guerra, Alberto, Tosetti, Michela, 2007. Age Dependence of Cerebral Perfusion Assessed by Magnetic Resonance Continuous Arterial Spin Labeling. J. Magn. Reson. Imaging.: JMRI 25 (4), 696–702. https://doi.org/10.1002/jmri.20839.

Bowman, Gene L., Dayon, Loïc, Kirkland, Richard, Wojcik, J.érôme, Peyratout, Gwendoline, Severin, India C., Henry, Hugues, et al., 2018. Blood-Brain Barrier Breakdown, Neuroinflammation, and Cognitive Decline in Older Adults. Alzheimer'S. Dement.: J. Alzheimer'S. Assoc. 14 (12), 1640–1650. https://doi.org/10.1016/j.jalz.2018.06.2857.

Chappell, Michael A., Groves, Adrian R., Whitcher, Brandon, Woolrich, Mark W., 2009. Variational Bayesian Inference for a Nonlinear Forward Model. IEEE Trans. Signal Process.: A Publ. IEEE Signal Process. Soc. 57 (1), 223–236. https://doi.org/10.1109/TSP.2008.2005752.

Clement, Patricia, Mutsaerts, Henk-Jan, Václavů, Lena, Ghariq, Eidrees, Pizzini, Francesca B., Smits, Marion, Acou, Marjan, et al., 2017. Variability of physiological brain perfusion in healthy subjects - A systematic review of modifiers. Considerations for multi-center ASL studies. January, 271678X17702156 J. Cereb. Blood Flow. Metab.: Off. J. Int. Soc. Cereb. Blood Flow. Metab.. https://doi.org/10.1177/0271678X17702156.

Clement, Patricia, Petr, Jan, Dijsselhof, Mathijs B.J., Padrela, Beatriz, Pasternak, Maurice, Dolui, Sudipto, Jarutyte, Lina, et al., 2022. A Beginner's Guide to Arterial Spin Labeling (ASL) Image Processing. Front. Radiol. 2. https://doi.org/10.3389/fradi.2022.929533.

Daneman, Richard, Prat, Alexandre, 2015. The Blood-Brain Barrier. Cold Spring Harb. Perspect. Biol. 7 (1), a020412. https://doi.org/10.1101/cshperspect.a020412.

Elschot, Elles P., Backes, Walter H., Postma, Alida A., van Oostenbrugge, Robert J., Staals, Julie, Rouhl, Rob P.W., Jansen, Jacobus F.A., 2021. A Comprehensive View on MRI Techniques for Imaging Blood-Brain Barrier Integrity. Invest. Radiol. 56 (1), 10–19. https://doi.org/10.1097/RLI.0000000000000723.

Fallatah, S.M., Pizzini, F.B., Gomez-Anson, B., Magerkurth, J., De Vita, E., Bisdas, S., Jäger, H.R., Mutsaerts, H.J.M.M., Golay, X., 2018. A Visual Quality Control Scale for Clinical Arterial Spin Labeling Images. Eur. Radiol. Exp. 2 (1), 45. https://doi.org/10.1186/s41747-018-0073-2.

Ford, Jeremy N., Zhang, Qihao, Sweeney, Elizabeth M., Merkler, Alexander E., de Leon, Mony J., Gupta, Ajay, Nguyen, Thanh D., Ivanidze, Jana, 2022. Quantitative Water Permeability Mapping of Blood-Brain-Barrier Dysfunction in Aging. Front. Aging Neurosci. 14 (April), 867452. https://doi.org/10.3389/fnagi.2022.867452.

Gold, Brian T., Shao, Xingfeng, Sudduth, Tiffany L., Jicha, Gregory A., Wilcock, Donna M., Seago, Elayna R., Wang, Danny J.J., 2021. Water Exchange Rate across the Blood-Brain Barrier Is Associated with CSF Amyloid-β 42 in Healthy Older Adults. Alzheimer'S. Dement.: J. Alzheimer'S. Assoc. 17 (12), 2020–2029. https://doi.org/10.1002/alz.12357.

Goodall, E.F., Wang, C., Simpson, J.E., Baker, D.J., Drew, D.R., Heath, P.R., Saffrey, M.J., Romero, I.A., Wharton, S.B., 2018. Age-Associated Changes in the Blood-Brain Barrier: Comparative Studies in Human and Mouse. Neuropathol. Appl. Neurobiol. 44 (3), 328–340. https://doi.org/10.1111/nan.12408.

Gregori, Johannes, Schuff, Norbert, Kern, Rolf, Günther, Matthias, 2013. T2-Based Arterial Spin Labeling Measurements of Blood to Tissue Water Transfer in Human Brain. J. Magn. Reson. Imaging.: JMRI 37 (2), 332–342. https://doi.org/10.1002/jmri.23822.

Günther, Matthias, Oshio, Koichi, Feinberg, David A., 2005. Single-Shot 3D Imaging Techniques Improve Arterial Spin Labeling Perfusion Measurements. Magn. Reson. Med.: Off. J. Soc. Magn. Reson. Med. / Soc. Magn. Reson. Med. 54 (2), 491–498. https://doi.org/10.1002/mrm.20580.

Hafdi, Melanie, Mutsaerts, Henk Jmm, Petr, Jan, Richard, Edo, van Dalen, Jan Willem, 2022. Atherosclerotic Risk Is Associated with Cerebral Perfusion - A Cross-Sectional Study Using Arterial Spin Labeling MRI. NeuroImage. Clin. 36 (August), 103142. https://doi.org/10.1016/j.nicl.2022.103142.

Han, Hualu, Ning, Zihan, Yang, Dandan, Yu, Miaoxin, Qiao, Huiyu, Chen, Shuo, Chen, Zhensen, et al., 2022. Associations between Cerebral Blood Flow and Progression of White Matter Hyperintensity in Community-Dwelling Adults: A Longitudinal Cohort Study. Quant. Imaging Med. Surg. 12 (8), 4151–4165. https://doi.org/10.21037/qims-22-141.

Holme, Nathalie Linn Anikken, Zilakos, Ilias, Elstad, Maja, Skytioti, Maria, 2023. Cerebral Blood Flow Response to Cardiorespiratory Oscillations in Healthy Humans. Auton. Neurosci.: Basic Clin. 245 (March), 103069. https://doi.org/10.1016/j.autneu.2022.103069.

Hoshi, Akihiko, Yamamoto, Teiji, Shimizu, Keiko, Ugawa, Yoshikazu, Nishizawa, Masatoyo, Takahashi, Hitoshi, Kakita, Akiyoshi, 2012. Characteristics of Aquaporin Expression Surrounding Senile Plaques and Cerebral Amyloid Angiopathy in Alzheimer Disease. J. Neuropathol. Exp. Neurol. 71 (8), 750–759. https://doi.org/10.1097/NEN.0b013e3182632566.

Hu, Ying, Liu, Rongbo, Gao, Fabao, 2021. Arterial Spin Labeling Magnetic Resonance Imaging in Healthy Adults: Mathematical Model Fitting to Assess Age-Related Perfusion Pattern. Korean J. Radiol.: Off. J. Korean Radiol. Soc. 22 (7), 1194–1202. https://doi.org/10.3348/kjr.2020.0716.

Hussain, Basharat, Fang, Cheng, Chang, Junlei, 2021. Blood-Brain Barrier Breakdown: An Emerging Biomarker of Cognitive Impairment in Normal Aging and Dementia. Front. Neurosci. 15 (August), 688090. https://doi.org/10.3389/fnins.2021.688090.

Juttukonda, Meher R., Li, Binyin, Almaktoum, Randa, Stephens, Kimberly A., Yochim, Kathryn M., Yacoub, Essa, Buckner, Randy L., Salat, David H., 2021. Characterizing Cerebral Hemodynamics across the Adult Lifespan with Arterial Spin Labeling MRI Data from the Human Connectome Project-Aging. NeuroImage 230 (April), 117807. https://doi.org/10.1016/j.neuroimage.2021.117807.

Klatsky, Arthur L., Zhang, Jasmine, Udaltsova, Natalia, Li, Yan, Tran, H.Nicole, 2017. Body Mass Index and Mortality in a Very Large Cohort: Is It Really Healthier to Be Overweight? Perm. J. 21, 16–142. https://doi.org/10.7812/TPP/16-142.

Kress, Benjamin T., Iliff, Jeffrey J., Xia, Maosheng, Wang, Minghuan, Wei, Helen S., Zeppenfeld, Douglas, Xie, Lulu, et al., 2014. Impairment of Paravascular Clearance Pathways in the Aging Brain. Ann. Neurol. 76 (6), 845–861. https://doi.org/10.1002/ana.24271.

Lindner, Thomas, Bolar, Divya S., Achten, Eric, Barkhof, Frederik, Bastos-Leite, António J., Detre, John A., Golay, Xavier, et al., 2023. Current State and Guidance on Arterial Spin Labeling Perfusion MRI in Clinical Neuroimaging. Magn. Reson. Med.: Off. J. Soc. Magn. Reson. Med. / Soc. Magn. Reson. Med. 89 (5), 2024–2047. https://doi.org/10.1002/mrm.29572.

Liu, Hua-Shan, Jawad, Abbas F., Laney, Nina, Hartung, Erum A., Furth, Susan L., Detre, John A., 2019. Effect of Blood T1 Estimation Strategy on Arterial Spin Labeled Cerebral Blood Flow Quantification in Children and Young Adults with Kidney Disease. J. Neuroradiol. J. De. Neuroradiol. 46 (1), 29–35. https://doi.org/10.1016/j.neurad.2018.03.002.

Liu, Wenjia, Lou, Xin, Ma, Lin, 2016. Use of 3D Pseudo-Continuous Arterial Spin Labeling to Characterize Sex and Age Differences in Cerebral Blood Flow. Neuroradiology 58 (9), 943–948. https://doi.org/10.1007/s00234-016-1713-y.

Liu, Yinan, Zhu, Xiaoping, Feinberg, David, Guenther, Matthias, Gregori, Johannes, Weiner, Michael W., Schuff, Norbert, 2012. Arterial Spin Labeling MRI Study of Age and Gender Effects on Brain Perfusion Hemodynamics. Magn. Reson. Med.: Off. J. Soc. Magn. Reson. Med. / Soc. Magn. Reson. Med. 68 (3), 912–922. https://doi.org/10.1002/mrm.23286.

Lorenzini, Luigi, Ansems, Loes T., Lopes Alves, Isadora, Ingala, Silvia, Vállez García, David, Tomassen, Jori, Sudre, Carole, et al., 2022. Regional Associations of White Matter Hyperintensities and Early Cortical Amyloid Pathology. Brain Commun. 4 (3). https://doi.org/10.1093/braincomms/fcac150.

Mahroo, Amnah, Buck, Mareike Alicja, Huber, J.örn, Breutigam, Nora-Josefin, Mutsaerts, Henk J.M.M., Craig, Martin, Chappell, Michael, Günther, Matthias, 2021. Robust Multi-TE ASL-Based Blood–Brain Barrier Integrity Measurements. Front. Neurosci. 15, 1549. https://doi.org/10.3389/fnins.2021.719676.

Mahroo, Amnah, Konstandin, Simon, Günther, Matthias, 2023. Blood-Brain Barrier Permeability to Water Measured Using Multiple Echo Time Arterial Spin Labeling MRI in the Aging Human Brain. *J. Magn. Reson. Imaging.: JMRI*, June. https://doi.org/10.1002/jmri.28874.

Moon, Yeonsil, Lim, Changmok, Kim, Yeahoon, Moon, Won-Jin, 2021. Sex-Related Differences in Regional Blood-Brain Barrier Integrity in Non-Demented Elderly Subjects. Int. J. Mol. Sci. 22 (6). https://doi.org/10.3390/ijms22062860.

Morgan, Catherine A., Thomas, David L., Shao, Xingfeng, Mahroo, Amnah, Manson, Tabitha J., Suresh, Vinod, Jansson, Deidre, et al., 2024. Measurement of Blood-Brain Barrier Water Exchange Rate Using Diffusion-Prepared and Multi-Echo Arterial Spin Labelling: Comparison of Quantitative Values and Age Dependence (September). NMR Biomed., e5256. https://doi.org/10.1002/nbm.5256.

Moyaert, Paulien, Padrela, Beatriz, Morgan, Catherine, Petr, Jan, Versijpt, Jan, Barkhof, Frederik, Jurkiewicz, Michael, et al., 2023. Imaging Blood-Brain Barrier Dysfunction: A State-of-the-Art Review from a Clinical Perspective. Front. Aging Neurosci. 15. https://doi.org/10.3389/fnagi.2023.1132077.

Mutsaerts, H.J.M.M., van Dalen, J.W., Heijtel, D.F.R., Groot, P.F.C., Majoie, C.B.L.M., Petersen, E.T., Richard, E., Nederveen, A.J., 2015. Cerebral Perfusion Measurements in Elderly with Hypertension Using Arterial Spin Labeling. PloS One 10 (8), e0133717. https://doi.org/10.1371/journal.pone.0133717.

Mutsaerts, Henri J.M.M., Petr, Jan, Bokkers, Reinoud P.H., Lazar, Ronald M., Marshall, Randolph S., Asllani, Iris, 2020b. Spatial Coefficient of Variation of Arterial Spin Labeling MRI as a Cerebrovascular Correlate of Carotid Occlusive Disease. PloS One 15 (2), e0229444. https://doi.org/10.1371/journal.pone.0229444.

Mutsaerts, Henk J.M.M., Petr, Jan, Groot, Paul, Vandemaele, Pieter, Ingala, Silvia, Robertson, Andrew D., Václavů, Lena, et al., 2020a. ExploreASL: An Image Processing Pipeline for Multi-Center ASL Perfusion MRI Studies (June). NeuroImage, 117031. https://doi.org/10.1016/j.neuroimage.2020.117031.

Mutsaerts, Henri J.M.M., Richard, Edo, Heijtel, Dennis F.R., van Osch, Matthias J.P., Majoie, Charles B.L.M., Nederveen, Aart J., 2014. Gray Matter Contamination in Arterial Spin Labeling White Matter Perfusion Measurements in Patients with Dementia. NeuroImage. Clin. 4, 139–144. https://doi.org/10.1016/j.nicl.2013.11.003.

Nation, Daniel A., Sweeney, Melanie D., Montagne, Axel, Sagare, Abhay P., D'Orazio, Lina M., Pachicano, Maricarmen, Sepehrband, Farshid, et al., 2019. Blood-Brain Barrier Breakdown Is an Early Biomarker of Human Cognitive Dysfunction. Nat. Med. 25 (2), 270–276. https://doi.org/10.1038/s41591-018-0297-y.

Ohene, Y., Harrison, I., Evans, P.E., Thomas, D.L., Lythgoe, M.F., Wells, J., 2020. Increased Blood-Brain Interface Permeability to Water in the Ageing Brain Detected Using Non-Invasive multi-TE ASL MRI (In press (In press): In press). Magn. Reson. Med.: Off. J. Soc. Magn. Reson. Med. / Soc. Magn. Reson. Med.. https://doi.org/10.1002/mrm.28496.

Ohene, Yolanda, Harrison, Ian F., Nahavandi, Payam, Ismail, Ozama, Bird, Eleanor V., Ottersen, Ole P., Nagelhus, Erlend A., Thomas, David L., Lythgoe, Mark F., Wells, Jack A., 2019. Non-Invasive MRI of Brain Clearance Pathways Using Multiple Echo Time Arterial Spin Labelling: An Aquaporin-4 Study. NeuroImage 188 (March), 515–523. https://doi.org/10.1016/j.neuroimage.2018.12.026.

Padrela, Beatriz, Mahroo, Amnah, Tee, Mervin, Sneve, Markus H., Moyaert, Paulien, Geier, Oliver, Kuijer, Joost P.A., et al., 2024. Developing Blood-Brain Barrier Arterial Spin Labelling as a Non-Invasive Early Biomarker of Alzheimer's Disease (DEBBIE-AD): A Prospective Observational Multicohort Study Protocol. BMJ Open 14 (3), e081635. https://doi.org/10.1136/bmjopen-2023-081635.

Petr, Jan, Mutsaerts, Henri J.M.M., Vita, Enrico De, Steketee, Rebecca M.E., Smits, Marion, Nederveen, Aart J., Hofheinz, Frank, Hoff, J.örg van den, Iris Asllani, 2018. Effects of Systematic Partial Volume Errors on the Estimation of Gray Matter Cerebral Blood Flow with Arterial Spin Labeling MRI. Magma 31 (6), 725–734. https://doi.org/10.1007/s10334-018-0691-y.

Pinto, Elisabete, 2007. Blood Pressure and Ageing. Postgrad. Med. J. 83 (976), 109–114. https://doi.org/10.1136/pgmj.2006.048371.

Ramalho, Miguel, Ramalho, Joana, Burke, Lauren M., Semelka, Richard C., 2017. Gadolinium Retention and Toxicity-An Update. Adv. Chronic Kidney Dis. 24 (3), 138–146. https://doi.org/10.1053/j.ackd.2017.03.004.

Robinson, Tyler D., Yutong, L.Sun, Chang, Paul T.H., Jean Chen, J., 2023. In Search of a Unifying Theory of White Matter Aging: Associations with Age in Perfusion Detectable in Advance of Microstructure. bioRxiv. https://doi.org/10.1101/2023.06.30.547294.

Robison, Lisa S., Gannon, Olivia J., Salinero, Abigail E., Zuloaga, Kristen L., 2019. Contributions of Sex to Cerebrovascular Function and Pathology. Brain Res. 1710 (May), 43–60. https://doi.org/10.1016/j.brainres.2018.12.030.

Rosenberg, Gary A., 2012. Neurological Diseases in Relation to the Blood-Brain Barrier. J. Cereb. Blood Flow. Metab.: Off. J. Int. Soc. Cereb. Blood Flow. Metab. 32 (7), 1139–1151. https://doi.org/10.1038/jcbfm.2011.197.

Setiadi, Anthony, Korim, Willian S., Elsaafien, Khalid, Yao, Song T., 2018. The Role of the Blood-Brain Barrier in Hypertension. Exp. Physiol. 103 (3), 337–342. https://doi.org/10.1113/EP086434.

Shao, Xingfeng, Jann, Kay, Ma, Samantha J., Yan, Lirong, Montagne, Axel, Ringman, John M., Zlokovic, Berislav V., Wang, Danny J.J., 2020. Comparison Between Blood-Brain Barrier Water Exchange Rate and Permeability to Gadolinium-Based Contrast Agent in an Elderly Cohort. Front. Neurosci. 14 (ember), 571480. https://doi.org/10.3389/fnins.2020.571480.

Shao, Xingfeng, Ma, Samantha J., Casey, Marlene, D'Orazio, Lina, Ringman, John M., Wang, Danny J.J., 2019. Mapping Water Exchange across the Blood-Brain Barrier Using 3D Diffusion-Prepared Arterial Spin Labeled Perfusion MRI. Magn. Reson. Med.: Off. J. Soc. Magn. Reson. Med. / Soc. Magn. Reson. Med. 81 (5), 3065–3079. https://doi.org/10.1002/mrm.27632.

Shao, Xingfeng, Shou, Qinyang, Felix, Kimberly, Ojogho, Brandon, Jiang, Xuejuan, Gold, Brian T., Herting, Megan M., et al., 2024. Age-Related Decline in Blood-Brain Barrier Function Is More Pronounced in Males than Females in Parietal and Temporal Regions. bioRxiv. https://doi.org/10.1101/2024.01.12.575463.

Shao, Xingfeng, Zhao, Chenyang, Shou, Qinyang, St Lawrence, Keith S., Wang, Danny J. J., 2023. Quantification of Blood-Brain Barrier Water Exchange and Permeability with Multidelay Diffusion-Weighted Pseudo-Continuous Arterial Spin Labeling. Magn. Reson. Med.: Off. J. Soc. Magn. Reson. Med. / Soc. Magn. Reson. Med. 89 (5), 1990–2004. https://doi.org/10.1002/mrm.29581.

Skillbäck, Tobias, Delsing, Louise, Synnergren, Jane, Mattsson, Niklas, Janelidze, Shorena, Nägga, Katarina, Kilander, Lena, et al., 2017. CSF/serum Albumin Ratio in Dementias: A Cross-Sectional Study on 1861 Patients. Neurobiol. Aging 59 (ember), 1–9. https://doi.org/10.1016/j.neurobiolaging.2017.06.028.

Solarz, Anna, Majcher-Maślanka, Iwona, Chocyk, Agnieszka, 2021. Effects of Early-Life Stress and Sex on Blood-Brain Barrier Permeability and Integrity in Juvenile and Adult Rats. Dev. Neurobiol. 81 (7), 861–876. https://doi.org/10.1002/dneu.22846.

Spolarics, Zoltán, 2007. The X-Files of Inflammation: Cellular Mosaicism of X-Linked Polymorphic Genes and the Female Advantage in the Host Response to Injury and Infection. Shock 27 (6), 597–604. https://doi.org/10.1097/SHK.0b013e31802e40bd.

Staffaroni, Adam M., Cobigo, Yann, Elahi, Fanny M., Casaletto, Kaitlin B., Walters, Samantha M., Wolf, Amy, Lindbergh, Cutter A., Rosen, Howard J., Kramer, Joel H., 2019. A Longitudinal Characterization of Perfusion in the Aging Brain and Associations with Cognition and Neural Structure. Hum. Brain Mapp. 40 (12), 3522–3533. https://doi.org/10.1002/hbm.24613.

Sweeney, Melanie D., Montagne, Axel, Sagare, Abhay P., Nation, Daniel A., Schneider, Lon S., Chui, Helena C., Harrington, Michael G., et al., 2019. Vascular Dysfunction-The Disregarded Partner of Alzheimer's Disease. Alzheimer'S. Dement.: J. Alzheimer'S. Assoc. 15 (1), 158–167. https://doi.org/10.1016/j.jalz.2018.07.222.

Tarumi, Takashi, Shah, Furqan, Tanaka, Hirofumi, Haley, Andreana P., 2009. Association Between Central Elastic Artery Stiffness and Cerebral Perfusion in Deep Subcortical Gray and White Matter. Am. J. Hypertens. 24 (10), 1108–1113. https://doi.org/10.1038/ajh.2011.101.

Tibbling, G., Link, H., Ohman, S., 1977. Principles of Albumin and IgG Analyses in Neurological Disorders. I. Establishment of Reference Values. Scand. J. Clin. Lab. Investig. 37 (5), 385–390. https://doi.org/10.1080/00365517709091496.

Tombaugh, T.N., McIntyre, N.J., 1992. The Mini-Mental State Examination: A Comprehensive Review. J. Am. Geriatr. Soc. 40 (9), 922–935. https://doi.org/10.1111/j.1532-5415.1992.tb01992.x.

Tomoto, Tsubasa, Lu, Marilyn, Khan, Ayaz M., Liu, Jie, Pasha, Evan P., Tarumi, Takashi, Zhang, Rong, 2023. Cerebral Blood Flow and Cerebrovascular Resistance across the Adult Lifespan: A Multimodality Approach. J. Cereb. Blood Flow. Metab.: Off. J. Int. Soc. Cereb. Blood Flow. Metab. 43 (6), 962–976. https://doi.org/10.1177/0271678X231153741.

Uemura et al, M. n.d. Brain Microvascular Pericytes in Vascular Cognitive Impairment and Dementia. Accessed October 7, 2024. doi: 10.3389/fnagi.2020.00080. https://click.endnote.com/viewer?doi= 10.3389%2Ffnagi.2020.00080&token=WzM1NjQ3NTYsIjEwLjMzODkvZm5hZ2kuMjAyMC4wMDA4MCJd.GDqFZpRRL-xSKUVj97Pm3QH0jqM.

Verheggen, Inge C.M., de Jong, Joost J.A., van Boxtel, Martin P.J., Gronenschild, Ed.H.B. M., Palm, Walter M., Postma, Alida A., Jansen, Jacobus F.A., Verhey, Frans R.J., Backes, Walter H., 2020. Increase in Blood-Brain Barrier Leakage in Healthy, Older Adults. GeroScience 42 (4), 1183–1193. https://doi.org/10.1007/s11357-020-00211-2.

Verheggen, I.C.M., Van Boxtel, M.P.J., Verhey, F.R.J., Jansen, J.F.A., Backes, W.H., 2018. Interaction between Blood-Brain Barrier and Glymphatic System in Solute Clearance. Neurosci. Biobehav. Rev. 90 (July), 26–33. https://doi.org/10.1016/j.neubiorev.2018.03.028.

Vidorreta, Marta, Balteau, Evelyne, Wang, Ze, De Vita, Enrico, Pastor, María a, Thomas, David L., Detre, John a, Fernández-Seara, María a, 2014. Evaluation of segmented 3D acquisition schemes for whole-brain high-resolution arterial spin labeling at 3 T. NMR Biomed. 27 (11), 1387–1396. https://doi.org/10.1002/nbm.3201.

Vidyasagar, Rishma, Greyling, Arno, Draijer, Richard, Corfield, Douglas R., Parkes, Laura M., 2013. The Effect of Black Tea and Caffeine on Regional Cerebral Blood Flow Measured with Arterial Spin Labeling. J. Cereb. Blood Flow. Metab.: Off. J. Int. Soc. Cereb. Blood Flow. Metab. 33 (6), 963–968. https://doi.org/10.1038/jcbfm.2013.40.

Wamelink, Ivar J.H.G., Azizova, Aynur, Booth, Thomas C., Mutsaerts, Henk J.M.M., Ogunleye, Afolabi, Mankad, Kshitij, Petr, Jan, Barkhof, Frederik, Keil, Vera C., 2024. Brain Tumor Imaging without Gadolinium-Based Contrast Agents: Feasible or Fantasy? Radiology 310 (2), e230793. https://doi.org/10.1148/radiol.230793.

Wang, Yunpeng, Grydeland, H.åkon, Roe, James M., Pan, Mengyu, Magnussen, Fredrik, Amlien, Inge K., Watne, Leiv Otto, et al., 2022. Associations of Circulating C-Reactive Proteins, APOE ε4, and Brain Markers for Alzheimer's Disease in Healthy Samples across the Lifespan. Brain, Behav., Immun. 100 (February), 243–253. https://doi.org/10.1016/j.bbi.2021.12.008.

Weber, Callie M., Clyne, Alisa Morss, 2021. Sex Differences in the Blood-Brain Barrier and Neurodegenerative Diseases. APL Bioeng. 5 (1), 011509. https://doi.org/10.1063/5.0035610.

Weiss, Nicolas, Miller, Florence, Cazaubon, Sylvie, Couraud, Pierre-Olivier, 2009. The Blood-Brain Barrier in Brain Homeostasis and Neurological Diseases. Biochim. Et. Biophys. Acta 1788 (4), 842–857. https://doi.org/10.1016/j.bbamem.2008.10.022.

Woods, Joseph G., Achten, Eric, Asllani, Iris, Bolar, Divya S., Dai, Weiying, Detre, John A., Fan, Audrey P., et al., 2024. Recommendations for Quantitative Cerebral Perfusion MRI Using Multi-Timepoint Arterial Spin Labeling: Acquisition, Quantification, and Clinical Applications. Magn. Reson. Med.: Off. J. Soc. Magn. Reson. Med. / Soc. Magn. Reson. Med. 92 (2), 469–495. https://doi.org/10.1002/mrm.30091.

Yang, Jing, Lunde, Lisa K., Nuntagij, Paworn, Oguchi, Tomohiro, Camassa, Laura M.A., Nilsson, Lars N.G., Lannfelt, Lars, et al., 2011. Loss of Astrocyte Polarization in the Tg-ArcSwe Mouse Model of Alzheimer's Disease. J. Alzheimer'S. Dis.: JAD 27 (4), 711–722. https://doi.org/10.3233/JAD-2011-110725.

Yang, Wei, Wu, Qi, Yuan, Chan, Gao, Junying, Xiao, Ming, Gu, Minxia, Ding, Jiong, Hu, Gang, 2012. Aquaporin-4 Mediates Astrocyte Response to β-Amyloid. Mol. Cell. Neurosci. 49 (4), 406–414. https://doi.org/10.1016/j.mcn.2012.02.002.

Zeppenfeld, Douglas M., Simon, Matthew, Haswell, J.Douglas, D'Abreo, Daryl, Murchison, Charles, Quinn, Joseph F., Grafe, Marjorie R., Woltjer, Randall L., Kaye, Jeffrey, Iliff, Jeffrey J., 2017. Association of Perivascular Localization of Aquaporin-4 With Cognition and Alzheimer Disease in Aging Brains. JAMA Neurol. 74 (1), 91–99. https://doi.org/10.1001/jamaneurol.2016.4370.